

Incommensurate Chiral CDW in $1T\text{-VSe}_2$

Y. Sugawara¹, A. Nomura¹, Y. Toda¹, T. Kurosawa²,

M. Oda², T. Matsuura¹, K. Ichimura¹, and S. Tanda¹

¹*Department of Applied Physics, Hokkaido University and*

²*Department of Physics, Hokkaido University*

(Dated: December 17, 2018)

ABSTRACT

We have investigated the chiral charge-density wave (CDW) in $1T$ -VSe₂ using scanning tunneling microscopy (STM) measurements and optical polarimetry measurements. With the STM measurements, we revealed that the CDW intensities along each triple- q directions are different. Thus the rotational symmetry of $1T$ -VSe₂ is lower than that in typical two-dimensional triple- q CDWs. We found that the CDW peaks form a kagome lattice rather than a triangular lattice. The Friedel oscillations have the chirality and the periodicity reflected properties of the background CDW. With the optical measurements in $1T$ -VSe₂, we also observed a lower rotational symmetry with the polarization dependence of the transient reflectivity variation, which is consistent with the STM result on a microscopic scale. Both $1T$ -TiSe₂ and $1T$ -VSe₂ show chiral CDWs, which implies that such waves are usual for CDWs with the condition $H_{\text{CDW}} \equiv q_1 \cdot (q_2 \times q_3) \neq 0$.

INTRODUCTION

The concept of chirality has recently been receiving a lot of attention in many fields, including chiral condensates and chiral density waves [1] in quantum chromodynamics, chiral spin texture [2] and electrical magnetochiral anisotropy [3–5] in condensed matter physics,

cholesteric liquid crystal and chiral helimagnetic order in application fields, and more. In relation to superconductors, chiral p -wave superconductivity [6] is also attracting attention. In particular, it is suggested that the pseudogap state in a high temperature superconductor is related to chiral order [7, 8] and this property must be understood if we are to clarify the high- T_c superconductor mechanism. Thus chirality is related to many fields, from elementary particles to macroscopic phenomena.

In recent years, the chiral charge-density wave (CDW), which is a new class of two-dimensional triple- q CDW, was discovered in $1T$ -TiSe₂ [9, 10]. In transition metal dichalcogenides MX₂ such as $1T$ -TaS₂, which are well known as typical two-dimensional CDW materials [11], the intensities of CDW wave vectors q_1 , q_2 and q_3 have the same magnitude. However in chiral CDWs, these values are different. Hence, the structure of the charge distribution has a clockwise or anticlockwise intensity anisotropy, so that the symmetry in a chiral CDW is less than in other MX₂ CDWs. In other words, it is a system that is broken in terms of both inversion and rotational symmetry. This phenomenon has attracted a lot of attention as regards similarities between the high- T_c pseudogap state and charge-parity symmetry. A chiral CDW is believed to be a widespread phenomenon because it has also been observed in $2H$ -TaS₂ [12], but its characteristics are as yet known. H_{CDW} is cited as

the condition for CDW chirality and is defined as $H_{\text{CDW}} \equiv q_1 \cdot (q_2 \times q_3)$, where q_1 , q_2 and q_3 are the CDW q vectors or nesting vectors with c^* components in triple- q systems [9].

However, as yet there are no materials that fulfill the condition and can be confirmed to be a chiral CDW except for $1T$ -TiSe₂. Therefore it is necessary to elucidate the condition of the chiral CDW.

We note that the new material $1T$ -VSe₂ offers the potential for a chiral CDW. It is unique among MX₂ CDW materials because an X-ray diffraction measurement [13] confirmed that its CDW is commensurate in two-dimensional layers but incommensurate in the direction perpendicular to the layers. The CDW wave vector in the c^* direction is $0.314c^*$ above 85 K and $0.307c^*$ below 85 K [14]. These values are quite different from the commensurate value of $0.333c^*$. This difference cannot be explained from the mechanism whereby most of the MX₂ undergoes commensurate CDW in the interlayer direction by stacking to avoid the CDW peaks of each layer overlapping and thus benefit the Coulomb energy. Thus, with $1T$ -VSe₂, CDWs may be commensurate both in the layer direction and the interlayer directions. The Fermi surface of $1T$ -VSe₂ obtained by band calculations [15] and angle resolved photoemission spectroscopy [16, 17] suggests that its nesting vectors have c^* components. So its CDW is three-dimensional although $1T$ -VSe₂ is a two-dimensional layered material.

In this work, we investigated $1T$ -VSe₂ as regards the chirality. We found the chirality in the $1T$ -VSe₂ CDW by using scanning tunneling microscopy (STM) and optical polarimetry measurements. In the STM measurements, we found different intensity ratios for three CDW directions and the CDW peaks formed a kagome lattice. In optical polarimetry measurements, we found a lower two-fold symmetry in $1T$ -VSe₂ than in a typical two-dimensional triple- q CDW such as $1T$ -TaS₂. By analyzing STM images, we found that Friedel oscillations on chiral CDWs reflect the chirality and periodicity of the underlying CDW.

EXPERIMENTAL

The samples were grown by the chemical vapor transport method. The elements (vanadium rod and selenium flake) in evacuated silica tubes were heated at 750 for 5 days. We obtained single crystals of $1T$ -VSe₂, which were platelets as large as $2 \times 2 \times 0.1$ mm³.

In the STM measurements, the samples were cleaved in situ just before the STM tip approached the surface in an ultra high vacuum at 77 K and we obtained samples with clean surfaces. The STM images were obtained at 80 K and 8 K.

The pump-probe pulse method was employed with the sample surface using the micro-

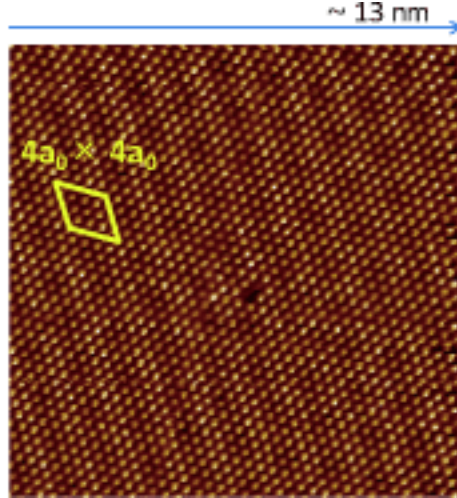


FIG. 1: 13 nm \times 13 nm STM image measured in situ at a sample voltage of $V = -100$ mV and an initial tunneling current of $I = 2.0$ nA at 80 K. The spots correspond to Se atoms and the brightness corresponds to local electron density. The orange parallelogram indicates the $4a_0 \times 4a_0$ CDW superlattice.

optics at 4 K. The pump and probe pulse polarization was varied to investigate the dominant direction of the deviation of the reflectivity $\Delta R(t)$.

RESULTS AND DISCUSSION

Figure 1 shows an STM current image obtained at the a - b plane of $1T$ -VSe₂ at 80 K. The CDW transition temperature of $1T$ -VSe₂ is 110 K [18], so this image shows the electronic property below the CDW transition temperature. The spots correspond to Se atoms and the brightness represents the magnitude of the local electron density. We can observe the periodic modulation of the electron density over the entire image. It has a $4a_0 \times 4a_0$ periodicity indicated by the orange parallelogram in Fig. 1. This periodicity corresponds to the

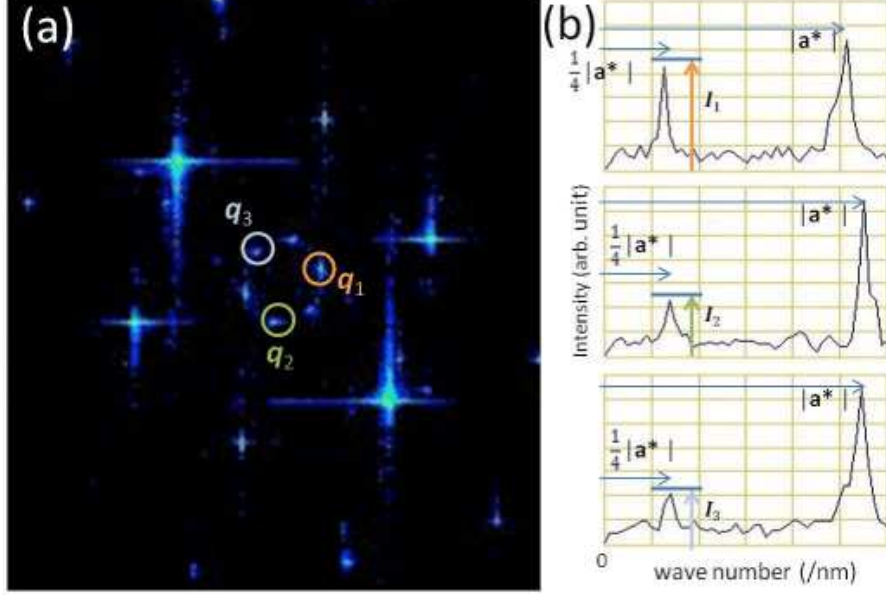


FIG. 2: (a) Fourier transformation (FT) image of Fig. 1. The spots surrounded by circles show the CDW wave vectors q_1 , q_2 and q_3 . (b) Line profiles along the q_1 , q_2 and q_3 wave vectors. I_1 , I_2 and I_3 show the intensities of each CDW peak. FT was performed over the entire field of view (13 nm \times 13 nm) of the STM image.

$4a_0$ CDW superlattice, which is consistent with a report that employed X-ray diffraction measurements[14]. However, compared with a typical two-dimensional triple- q CDW, such as $1T$ -TaS₂, this CDW structure appears to be different because there is a difference in brightness that corresponds to the CDW intensity in each CDW direction.

To investigate that periodic structure, we analyzed a Fourier transformation (FT) image of the STM. Figure 2(a) shows an FT image of the entire field of Fig. 1. The bright spots surrounded by circles correspond to CDW vectors q_1 , q_2 and q_3 . The outer intensity peaks correspond to the Bragg peaks of the selenium lattice, and the inner peaks correspond to

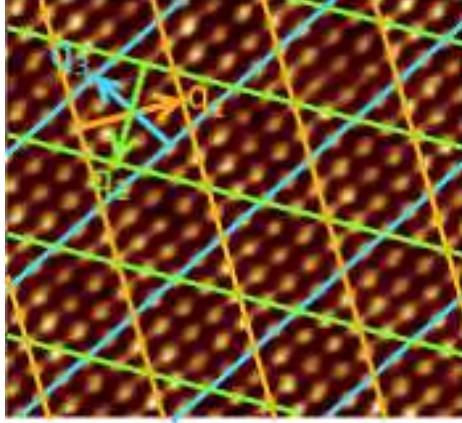


FIG. 3: Enlarged view of a portion of Fig. 1. The orange lines show the strongest intensity of the CDW. The green and blue lines show the second strongest and weakest intensities of the CDW peak, respectively. The lines form a kagome lattice.

the CDW satellite peaks. Figure 2(b) shows line profiles of an FT image along the q_1 , q_2 and q_3 wave vector. I_n ($n = 1, 2, 3$) represents the intensity of CDW satellite peaks along each wave vector. We found an obvious difference between the CDW intensities of CDW vectors q_1 , q_2 and q_3 ; I_1 is the strongest and I_2 and I_3 are the second strongest and weakest, respectively. In typical two-dimensional CDWs I_1 , I_2 and I_3 must be of equal value and the CDW structure is expected to have six-fold symmetry. However in $1T$ -VSe₂ each I_n is different, so the CDW of $1T$ -VSe₂ has lower symmetry. We concluded that is a chiral CDW by analyzing an FT image and decided that the CDW structure is clockwise because the direction from q_1 to q_2 to q_3 in descending order of the magnitude of I_n is clockwise in an FT image as reported elsewhere [10].

Then we consider the CDW formation in real space from the result of an FT image. Figure 3 is an enlarged view of Fig. 1. The orange lines show the wave front of the strongest intensity CDW wave vector q_1 found in Fig. 2. The green and blue lines show the second strongest and weakest intensity CDW wave fronts of q_2 and q_3 , respectively. We found that the CDW peaks form a kagome lattice rather than a triangular lattice. Previous papers on STM observations of $1T$ -VSe₂ did not report on this matter[19–21]. The kagome lattice, which has an intensity difference, has two-fold symmetry. This is unlike a conventional kagome lattice, which has three-fold symmetry and no mirror symmetry. As a result of the lower symmetry mentioned above, we conclude that the CDW on $1T$ -VSe₂ is also a chiral CDW in real space.

Secondly, we measured the polarization dependence of the transient reflectivity of $1T$ -VSe₂ by using the pump-probe method to investigate the macroscopic symmetry. With an optical measurement using a probe light whose penetration length is several tens of nanometers, we can measure the symmetry of more deeper samples than that with an STM. Figure 4 shows the polarization dependence of the transient reflectivity variation of $1T$ -VSe₂ at 4 K. The heights of the peak intensities of each polarization angle in Fig. 4 (a) are plotted in Fig. 4 (b). The transient variation in optical reflectance $\Delta R(t)$ was measured by changing

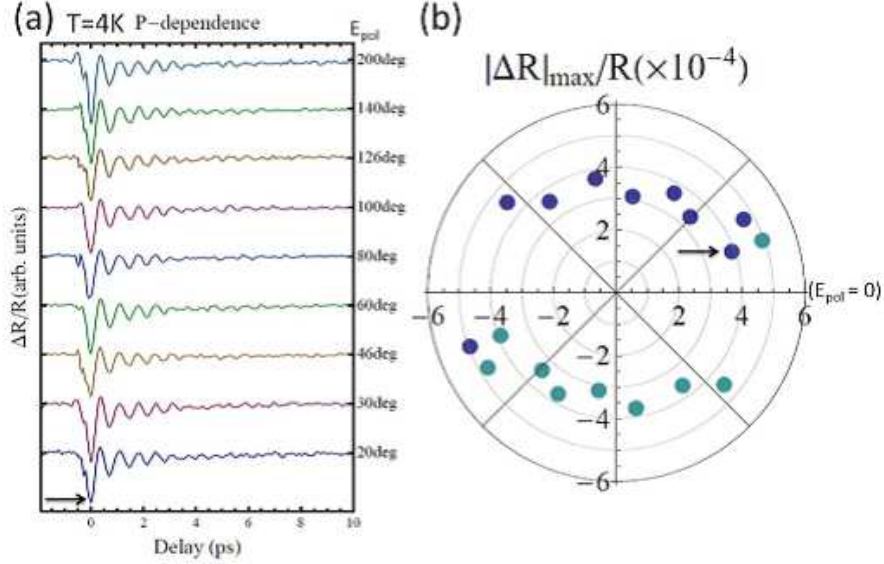


FIG. 4: (a) Polarization dependence of transient reflectivity variation in $1T$ -VSe₂ measured at 4 K. The height of each peak is plotted in (b) as a function of polarization angle. The amplitude indicated by the black arrows in (a) correspond to the spot indicated in (b).

the polarization angle E_{pol} of the incident probe laser pulse. In general, the peak intensity of transient signals corresponds to the number of electrons excited over the CDW gap [22, 23].

Figure 4 (b) shows that $1T$ -VSe₂ exhibits two-fold symmetry despite the crystal structure being a triangular lattice. For this reason, this result reflects the CDW characteristics as two-fold symmetry. That is similar to the result with $1T$ -TiSe₂ [9] and consistent with the result of the STM measurement on a microscopic scale. We also confirmed that the CDW in $1T$ -VSe₂ is a chiral CDW with an optical polarimetry measurement.

Next, we analyzed the charge density modulation around the charge impurities such as the lattice defects and adatoms observed in the STM measurements. Such modulations are

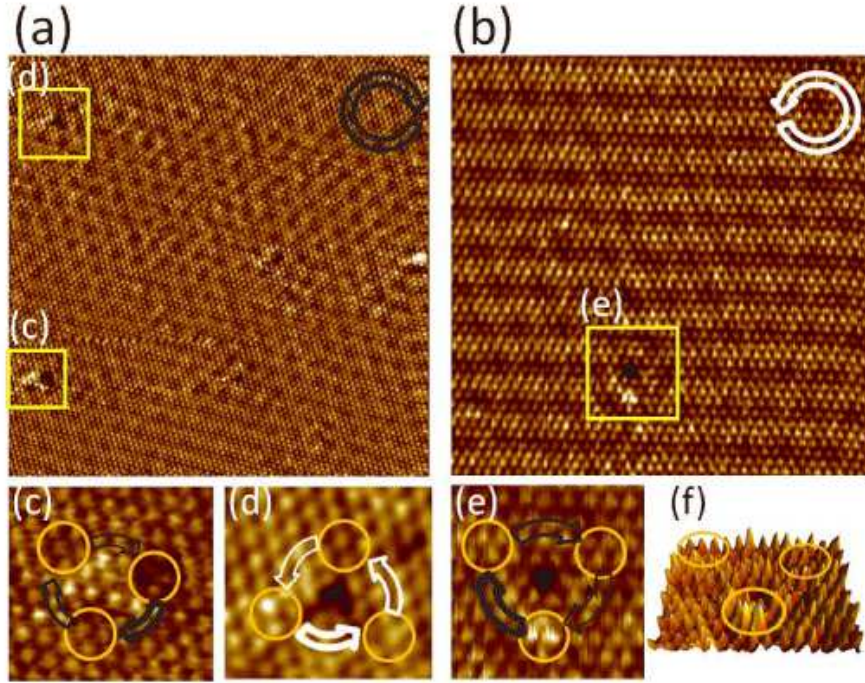


FIG. 5: (a) 24 nm \times 24 nm STM image measured at 80 K in the clockwise CDW. (b) 14 nm \times 14 nm STM image measured at 8 K in the counterclockwise CDW. The Friedel oscillations in the clockwise CDW [(c) and (e)] and counterclockwise CDW (d). Each peak and gap is indicated by orange circles. The black and the white arrows indicate clockwise and counterclockwise CDWs and FOs, respectively. (f) Three-dimensional plots of (e).

called Friedel Oscillations (FOs). FOs are damped oscillations whose wave number is Fermi wave number k_F , so an analysis of the FOs in CDW systems is important for the elucidation of CDW characteristics. Figures. 5 show the results analyzed the current images. The chirality of the underlying CDW is obtained by the process used in Fig. 2. Figure 5(a) is an STM image obtained in a clockwise CDW and Figure 5(b) shows an STM image obtained in a counterclockwise CDW. We observe the dark FO around a bright spot whose charge density is rich has clockwise chirality in a clockwise CDW in Fig. 5(c), while the bright

FO around a dark spot whose charge density is poor has counterclockwise chirality in the clockwise CDW in Fig. 5(d). Furthermore, we found that the bright FO around the dark spot has clockwise chirality in the counterclockwise CDW. That is, the chiralities of bright and dark FOs are the same and the opposite of the underlying CDW, respectively. We cannot observe any opposite chirality relationship between an underlying CDW and FOs in Fig 5(b). In the previous study of chiral CDWs in $1T$ -TiSe₂, dark FOs around the bright spot also have the opposite chirality and bright FOs around the dark spot also have the same chirality as the underlying CDW[10]. Thus the chirality of FOs in $1T$ -VSe₂ is the same as those in $1T$ -TiSe₂, but the periodicity of FOs in $1T$ -VSe₂ is longer than those in $1T$ -TiSe₂ because the CDW periodicities of $1T$ -VSe₂ and $1T$ -TiSe₂ are $4a_0$ and 2_0 , respectively. We found that the chirality of FOs reflects the underlying CDW chirality and periodicity.

Finally, we discuss the condition of the chiral CDW. Figure 6 shows the details of a CDW in the $1T$ -MSe₂ group (M = Ta, Ti, V). These CDWs have the same characteristics as a CDW with commensurate in a layer but they are quite different in the c^* direction. The CDW c^* superlattice of $1T$ -TaSe₂ is $3c_0$, which originates from CDW stacking, and this structure does not relate to the direction of the nesting vectors. Most triple- q CDW systems such as $1T$ -TaS₂ have a similar structure to $1T$ -TaSe₂. In $1T$ -TiSe₂, the c^* component

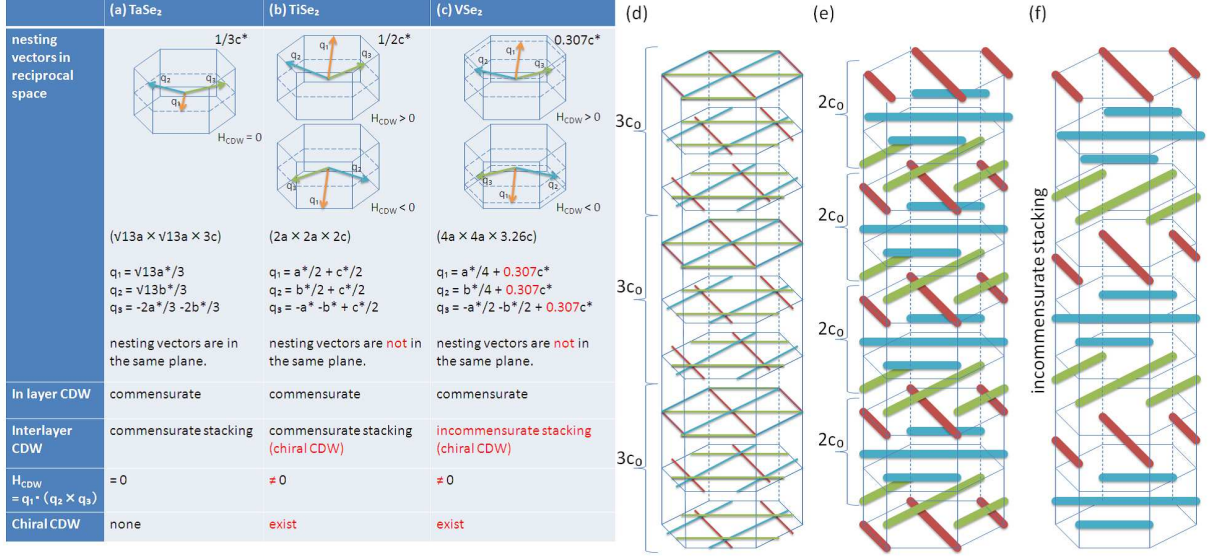


FIG. 6: Table showing details of the CDW in $1T$ -MSe₂ group (M = Ta, Ti, and V) [(a),(b), and (c)] and a schematic representation of each material [(d), (e), and (f)]. We provide pictures of nesting vectors in reciprocal space, the values of each nesting vector, the commensurateness of layer and interlayer CDWs, the value of $H_{CDW} \equiv q_1 \cdot (q_2 \times q_3)$ and the existence of the chiral CDWs of (a) $1T$ -TaSe₂, (b) $1T$ -TiSe₂ and (c) $1T$ -VSe₂. (a) $1T$ -TaSe₂ is a typical two-dimensional CDW material and its nesting vectors are in the same plane, so $H_{CDW} = 0$. The superlattice is $3c_0$, which originated from the stacking. There is no chiral CDW. (b) The nesting vectors of $1T$ -TiSe₂ are not in the same plane, so $H_{CDW} \neq 0$. Its interlayer CDW is commensurate. There is a chiral CDW. (c) The nesting vectors of $1T$ -VSe₂ are not in the same plane, so $H_{CDW} \neq 0$. Its interlayer CDW is incommensurate. There is a chiral CDW. Schematic representations of (d) a typical two-dimensional CDW similar to $1T$ -TaSe₂ and chiral CDW in (e) $1T$ -TiSe₂ and (f) $1T$ -VSe₂. Each hexagon shows a layer of each material. Colored lines show the charge concentration and the colors correspond to the CDW q vectors in (a), (b) and (c).

is commensurate as with $1T$ -TaSe₂, but it forms a $2c_0$ superlattice originating from nesting vectors with a $c^*/2$ component. This $2c_0$ superlattice stacks in the c^* direction and forms a chiral CDW. Meanwhile, the $1T$ -VSe₂ CDW is unique in triple- q CDW systems as it is incommensurate along the c^* direction because the c^* component of its nesting vectors is

an irrational number [14]. We cannot consider $1T$ -VSe₂ as composing the stacking unit, so the chiral CDW structure would appear directly below the transition temperature. In this respect, $1T$ -VSe₂ is a more important chiral CDW material than $1T$ -TiSe₂. A chiral CDW was discovered in both $1T$ -TiSe₂ and $1T$ -VSe₂ but there is little difference between them. Nevertheless, $H_{\text{CDW}} \neq 0$ is probably a necessary condition of the chiral CDW.

CONCLUSIONS

We discovered a chiral CDW in $1T$ -VSe₂ by using STM measurements and optical polarimetry measurements and by analyzing of the FOs. We also discovered that the CDW peaks in $1T$ -VSe₂ form a kagome lattice. $1T$ -VSe₂ has a unique characteristic as an incommensurate CDW along the c^* direction, which is different from other MX₂ triple- q CDWs, but it can be treated in the same way as $1T$ -TiSe₂ in terms of $H_{\text{CDW}} \equiv q_1 \cdot (q_2 \times q_3) \neq 0$. These results strongly suggest that the chiral CDW is a general phenomenon that can occur in systems that fulfill the condition $H_{\text{CDW}} \neq 0$.

-
- [1] I. E. Frolov, V. Ch. Zhukovsky, and K. G. Klimenko, Phys. Rev. D **82**,076002(2010)
 - [2] P. Poushan, J. Seo, C. V. Parker, Y. S. Hor, D. Hsieh, D. Qian, A. Richardella, M. Z. Hasan, R. J. Cava, and A. Yazdani, Nature **460**,1106(2009)
 - [3] G. L. J. A. Rikken, J. Fölling, and P. Wyder, Phys. Rev. Lett. **87**,236602(2001)

- [4] V. Krstić, S. Roth, M. Burghard, K. Kern and G. L. J. A. Rikken, J. Chem. Phys. **117**,11315(2002)
- [5] F. Pop, P. Auban-Senzier, E. Canadell, G. L. J. A. Rikken, and N. Avarvari, Nat. Commun. **5**,3757(2014)
- [6] H. Nobukane, A. Tokumo, T. Matsuyama, and S. Tanda, Phys. Rev. B **83**,144502(2011)
- [7] P. Hosur, A. Kapitulnik, S. A. Kivelson, J. Orenstein, and S. Raghu, Phys. Rev. B **87**,115116(2013)
- [8] S. S. Pershoguba, K. Kechedzhi, and V. M. Yakovenko, Phys. Rev. Lett. **111**,047005(20013)
- [9] J. Ishioka, Y. H. Liu, T. Kurosawa, K. Ichimura, Y. Toda, M. Oda, and S. Tanda, Phys. Rev. Lett. **105**,176401(2010)
- [10] J. Ishioka, T. Fujii, K. Katono, K. Ichimura, T. Kurosawa, M. Oda, and S. Tanda, Phys. Rev. B **84**,245125(2011)
- [11] J. A. Wilson, F. J. Di Salvo, and S. Mahajan, Phys. Rev. Lett. **32**,882(1974)
- [12] I. Guillamón, H. Suderow, J. G. Rodrigo, S. Vieira, P. Rodière, L. Cario, E. Navarro-Moratalla, C. Martí-Gastaldo, and E. Coronado, New J. phys. **13**,103020(2010)
- [13] K. Tsutsumi, T. Sambongi, A. Toriumi, and S. Tanaka, J. Phys. Soc. Jpn. **49**,2(1980)
- [14] K. Tsutsumi, Phys. Rev. B **26**,10(1982)
- [15] A. Zunger et al, Phys. Rev. B **19**,6001(1979)
- [16] T. Sato, K. Terashima, S. Souma, H. Matsui, T. Takahashi, H. Yang, S. Wang, H. Ding, N. Maeda, and K. Hayashi, J. Phys. Soc. Jpn. **73**,3331(2004)
- [17] V. N. Strocov et al, Phys. Rev. Lett. **109**,086401(2012)
- [18] A. V. Skripov, D. S. sibirtsev, Yu G. Cherepanov, and B. A. Aleksashin, J. Phys.: Condens Matter **7**,4479(1995)
- [19] R. V. Coleman, B. giambattista, P. K. Hansma, A. Johnson, W. W. McNairy and C. G. Slough, Adv. Phys. **37**,559(1988)
- [20] B. giambattista, C. G. Slough, W. W. McNairy, and R. V. Coleman, Phys. Rev. B **41**,10082(1990)
- [21] J. J. Kim, C. Park, and H. Olin, J. Korean Phys. Soc. **31**,713(1997)
- [22] J. Demsar, K. Biljakovic, and D. Mihailovic, Phys. Rev. Lett. **83**,800(1999)
- [23] J. Demsar, L. Forro, H. Berger, and D. Mihailovic, Phys. Rev. B. **66**,041101(2002)